

Structure of the FKBP12-Rapamycin Complex Interacting with the Binding Domain of Human FRAP

Jungwon Choi,* Jie Chen, Stuart L. Schreiber, Jon Clardy†

Rapamycin, a potent immunosuppressive agent, binds two proteins: the FK506-binding protein (FKBP12) and the FKBP-rapamycin-associated protein (FRAP). A crystal structure of the ternary complex of human FKBP12, rapamycin, and the FKBP12-rapamycin-binding (FRB) domain of human FRAP at a resolution of 2.7 angstroms revealed the two proteins bound together as a result of the ability of rapamycin to occupy two different hydrophobic binding pockets simultaneously. The structure shows extensive interactions between rapamycin and both proteins, but fewer interactions between the proteins. The structure of the FRB domain of FRAP clarifies both rapamycin-independent and -dependent effects observed for mutants of FRAP and its homologs in the family of proteins related to the ataxia-telangiectasia mutant gene product, and it illustrates how a small cell-permeable molecule can mediate protein dimerization.

A dividing cell must pass various checkpoints as it proceeds through the cell cycle, and error-free division requires the ability to rectify DNA lesions (1, 2). The ataxia-telangiectasia mutant (ATM) gene product, the catalytic subunit of the DNA-dependent protein kinase, and the products of yeast genes such as TOR1, TOR2, and MEC1 (ESR1) are members of a family of large molecular size proteins that participate in cell cycle progression and checkpoints as well as in DNA repair and recombination (1–4). All members of the ATM family contain a COOH-terminal kinase domain (1–4), but no structural information is available for any domain of any family member. Human FRAP (rat RAFT), one member of this family, is a 289-kD protein that binds FKBP12-rapamycin, regulates p70 ribosomal protein S6 kinase, and is required for G₁ cell cycle progression in several cell types (5–7).

The potent immunosuppressive agents FK506 (8) and rapamycin (9–11) (Fig. 1A) share the same cellular target: the 12-kD FK506-binding protein, FKBP12 (12, 13). Although both rapamycin and FK506 bind to FKBP12 with high affinity [dissociation constant (K_d), 0.2 to 0.4 nM], they effect immunosuppression through different mechanisms. Whereas FK506 interrupts the signal from the T cell receptor, rapamycin interrupts the signal from the interleukin-2 receptor and the receptors for other cytokines and growth factors (14). Binding of similar molecules, such as FK506 and rapamycin,

to the same protein can disrupt different signals because the protein-ligand complexes, (not the individual components) are the active entities (14). FKBP12-FK506 inhibits calcineurin, a serine-threonine phosphatase (15), whereas FKBP12-rapamycin binds to FRAP (5). Thus, small cell-permeable molecules can induce proteins to associate in a manner similar to that by which growth factors (such as human growth hormone), cytokines (such as interleukin-2), and intracellular signaling proteins (such as GRB2) induce dimerization of signaling proteins. These naturally occurring inducers of dimerization have inspired the design of synthetic molecules that induce dimerization of intracellular proteins and result in the activation of cytoplasmic signaling pathways (16).

FK506 and rapamycin bind FKBP12 in a hydrophobic pocket, and an important feature of both FKBP12-ligand structures is the large fraction, ~50%, of ligand exposed on the exterior of the complex (17–19). A composite surface—a surface with contributions from both ligand (FK506 or rapamycin) and the protein (FKBP12)—mediates the interaction of the FKBP12-ligand complex with its target (14). Two independent x-ray structures of the ternary FKBP12-FK506-calcineurin complex show a composite binding surface with extensive contacts between FK506 and its protein partners as well as between the protein partners themselves (20, 21). We now present a 2.7 Å x-ray structure that shows how rapamycin mediates the heterodimerization of FKBP12 with FRAP.

Binding of FRAP to FKBP12-rapamycin ($K_d = 2$ nM) is mediated by a small domain, the FKBP12-rapamycin-binding (FRB) domain, that can be expressed as a 12-kD soluble protein (22). Crystals (23) of the ternary FKBP12-rapamycin-FRB complex were pre-

pared and the structure was solved (24) by a combination of molecular replacement (MR) with isomorphous replacement for a single anomalously scattering derivative (SIRAS) (Fig. 1, B and C). The resulting MR-SIRAS map was readily interpretable, and the structure was refined to a final R factor of 0.193 (8.0 to 2.7 Å data). The ternary complex has a roughly rectangular shape with overall dimensions of 60 Å by 45 Å by 35 Å. The two protein components are virtually the same size, and rapamycin is almost completely buried between them. The ternary complex features an extensive array of rapamycin-protein interactions in two binding pockets lined with aromatic residues. FKBP12 contains a large β sheet composed of five antiparallel β strands (17–19). A short amphipathic α helix is pressed against this sheet, and rapamycin binds in a hydrophobic pocket formed between the α helix and β sheet. Three loops—the 40s loop, which is a bulge in β5, the 50s loop connecting β5 to α, and the 80s loop connecting β2 to β3—surround and contribute to the binding pocket. In general, the structure of the FKBP12-rapamycin portion of the ternary complex does not differ from that of the binary FKBP12-rapamycin complex (18, 19), and the overall root-mean-square deviation between the binary and ternary complex is 1.14 Å for all atoms and 0.49 Å for main chain atoms.

The FRB domain of FRAP forms a four-helix bundle, a common structural motif in globular proteins (25). Its overall dimensions are 30 Å by 45 Å by 30 Å, and all four helices (α1 to α4) have short underhand connections similar to the cytochrome b₅₆₂ fold (26). The NH₂- and COOH-termini of the FRB domain are close to each other, suggesting that an FRB-type domain could be inserted into other protein chains. The longest helix, α3, has a 60° bend at Tyr²⁰⁷⁴, roughly one-third of the distance from its NH₂-terminus, and the α2 helix has a small region (Gly²⁰⁴⁹ to Leu²⁰⁵¹) that deviates from a standard α helix. Ignoring the first 10 residues of α3, all four helices are ~26 Å in length and comprise 16 to 19 residues. The α1 and α2 helices are almost parallel (interhelical angle of 22°), as are α3 and α4 (20°), whereas the crossing angles between the α1-α2 pair and the α3-α4 pair range from 30° to 60°. The parallel helices are also closer. Helices α1-α2 and α3-α4 show the shortest interhelical distances of 6.3 and 7.2 Å, respectively, whereas other closest interhelical contacts range from 10 to 14 Å. Most of the hydrophobic and aromatic residues are located in the interhelical regions, and the hydrophilic residues are exposed to solvent. The first and last helices of the bundle, α1 and α4, form a deep cleft near their crossing point, and this cleft, which is lined by six aromatic side chains, forms the hydrophobic

J. Choi and J. Clardy, Department of Chemistry, Baker Laboratory, Cornell University, Ithaca, NY 14853-1301, USA.

J. Chen and S. L. Schreiber, Howard Hughes Medical Institute and Department of Chemistry and Chemical Biology, Harvard University, Cambridge, MA 02138, USA.

*Present address: Department of Chemistry, Suwon University, Kyunggi 445-773, South Korea.

†To whom correspondence should be addressed.

pocket in which rapamycin binds.

Rapamycin interacts extensively with both FKBP12 and FRB. Its interactions with FKBP12 resemble those described for the binary complex and feature extensive contacts with conserved aromatic residues and five hydrogen bonds (18, 19). Trp⁵⁹ forms the base of the binding pocket and contacts the pipercolinyl ring (C2 to N7)—the most deeply buried portion of rapamycin. A total of 460 Å² (44%) of the solvent-accessible surface area of rapamycin is buried in FKBP12. Rapamycin also interacts with the FRB domain of FRAP through close contacts with aromatic residues, and a series of interactions along the triene arm of rapamycin (C16 to C23) involving Phe²⁰³⁹, Trp²¹⁰¹, Tyr²¹⁰⁵, and Phe²¹⁰⁸ appear especially important (Fig. 2). Ser²⁰³⁵, Leu²⁰³¹, Thr²⁰⁹⁸, Asp²¹⁰², and Tyr²⁰³⁸ also make contact with rapamycin. There are no hydrogen bonds in the FRB-rapamycin interaction, and 340 Å² (33%) of the solvent-accessible surface area of rapamycin participate in the interaction. A small, but important, conformational change in rapamycin is evident between the binary (FKBP12-rapamycin) and ternary (FKBP12-rapamycin-FRB) complexes. In crystal structures of uncomplexed rapamycin (27) and the FKBP12-rapamycin complex (18), the triene arm of rapamycin is planar, with the three double bonds fully conjugated. In the ternary complex, rotations of -15° about C18-C19 and 37° about C20-C21 slightly disrupt the conjugation and move the most deeply buried portion of rapamycin, the methyl group attached to C23, by 1.6 Å (Fig. 1). This conformational alteration of rapamycin avoids a close contact with Phe²¹⁰⁸ and places the deeply buried methyl group in a small crease between Phe²¹⁰⁸ and Leu²⁰³¹ (Fig. 2). The macrocyclic loop of rapamycin is eight carbon atoms larger than the corresponding loop in FK506, and the triene portion of rapamycin reduces the conformational flexibility of the loop and holds it away from the surface of FKBP12—it organizes the loop for binding into a deep pocket. Our analysis suggests that the limited flexibility of the triene arm might also be an important feature of the structure of rapamycin. If FK506 and rapamycin are overlaid, the much shorter loop of FK506 does not approach the binding pocket of the FRB domain of FRAP.

Although rapamycin interacts extensively with both protein partners, the extent to which the proteins interact with each other is relatively limited (Fig. 2). Two regions of the complex show interactions between the proteins: the 40s loop of FKBP12 with α4 of FRB, and the 80s loop of FKBP12 with the α1-α2 region of FRB. In the 40s-α4 interaction, the OH group of Tyr²¹⁰⁵ and the O atom of Lys⁴⁷ make a short contact and there is also a water-mediated salt bridge. In the other inter-

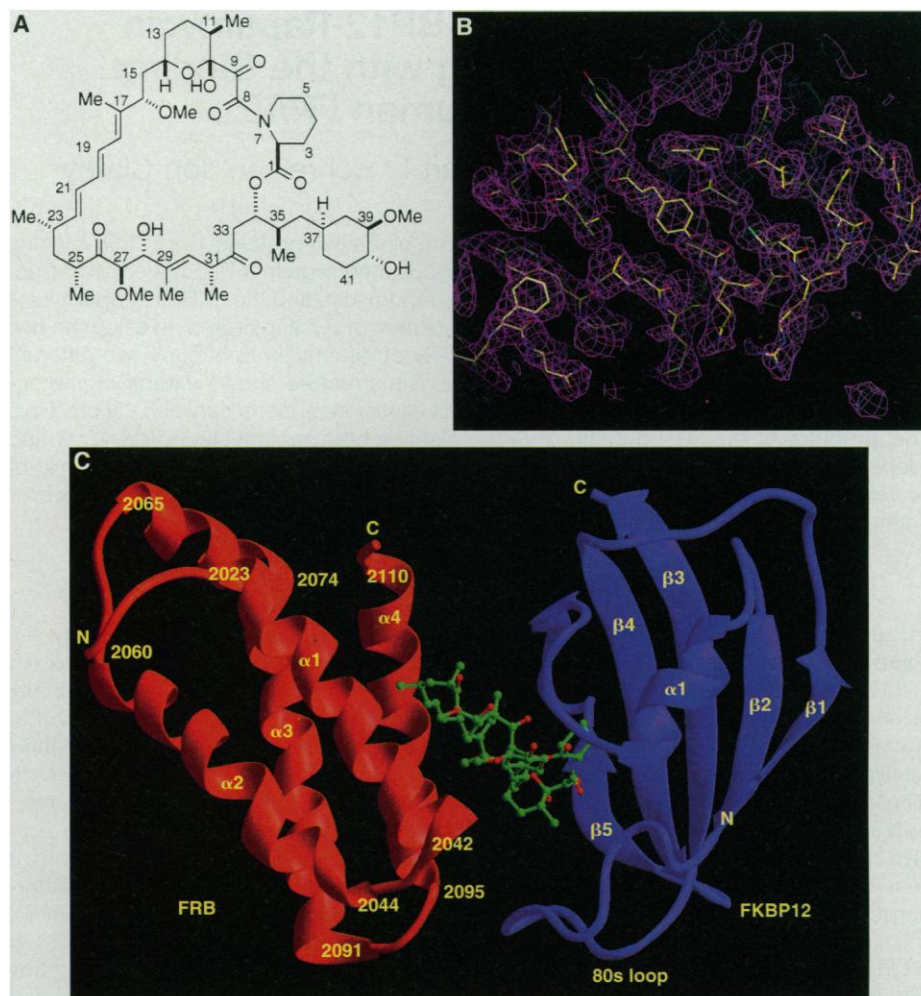


Fig. 1. (A) Chemical structure of rapamycin. (B) The $2F_o - F_c$ electron density of the FRB domain of the FKBP12-rapamycin-FRB complex (24) (F_o , observed structure factor; F_c , calculated structure factor). A model of the final structure is embedded in this initial electron density. (C) Overall structure of the ternary complex between FKBP12 (blue ribbon), rapamycin (ball and stick), and the FRB domain of FRAP (red ribbon). Secondary structural elements are labeled with the conventional numbering scheme for FKBP12. N and C, NH₂- and COOH-termini, respectively. The drawing in (C) was prepared with RIBBONS (37).

action region, the NH₂ group of Arg²⁰⁴² makes short contacts with Oγ1 of Thr⁸⁵ and the O atom of Gly⁸⁶, and there are two water-mediated interactions. Although the number of interprotein polar interactions is moderate, 400 Å² of solvent-accessible surface area, roughly equivalent to the surface area buried by FKBP12-rapamycin or FRB-rapamycin, participate in the interaction between them. The 80s loop of FKBP12 appears to be one region where the structure of FKBP12 differs between the binary and ternary complexes, with the major change being around Ile⁹⁰, where both side chain and main chain deviations are apparent. These deviations move FKBP12 away from the FRB domain, suggesting repulsion between the proteins in this region.

The residues that form the rapamycin binding pocket of FRAP (Fig. 2) are conserved in yeast Tor1p, Tor2p, and rat RAFT1—other ATM family members that

bind FKBP12-rapamycin—and thus all four proteins are likely to contain a hydrophobic pocket with similar architecture and related function. Overexpression of the Ser¹⁹⁷² (corresponding to Ser²⁰³⁵ of FRAP) → Ile mutant of Tor1p results in marked inhibition of cell growth that is dependent on the kinase activity of the mutant (28). These results indicate that the site bearing the Ser mutation may regulate the neighboring kinase domain of Tor1p (28). The conserved binding pocket associated with a regulatory function suggests that binding of an as yet unidentified ligand may regulate kinase activity. The shape of the binding pocket and the α1-α4 crossing angle are mutually dependent; thus, ligand binding could result in a change in the crossing angle, and the domain could function as a ligand-dependent conformational switch. FKBP12 might adjust the crossing angle (possibly by having its 80s loop repel the α1-α2 helical pair of the FRB domain of

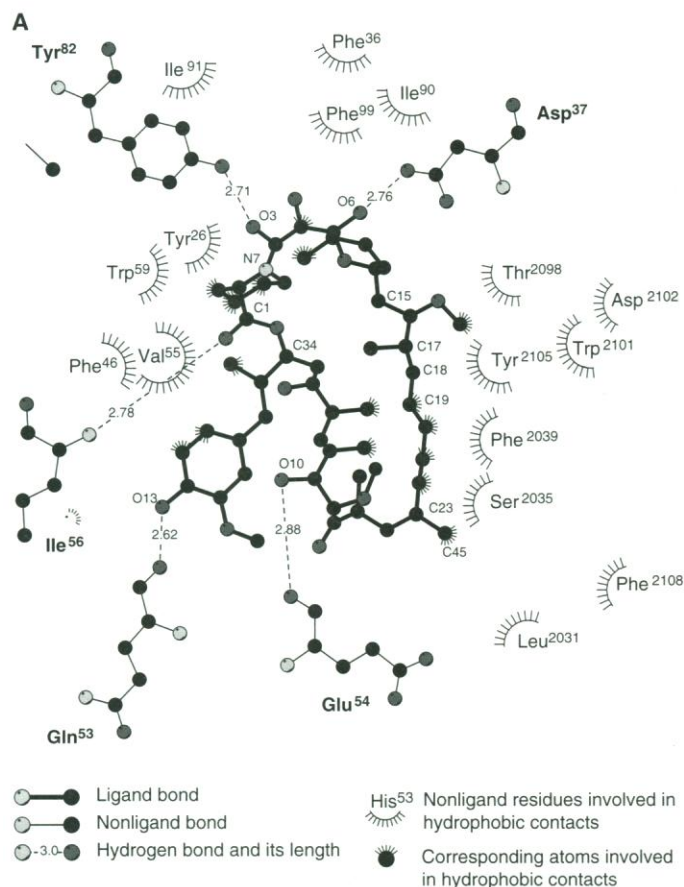
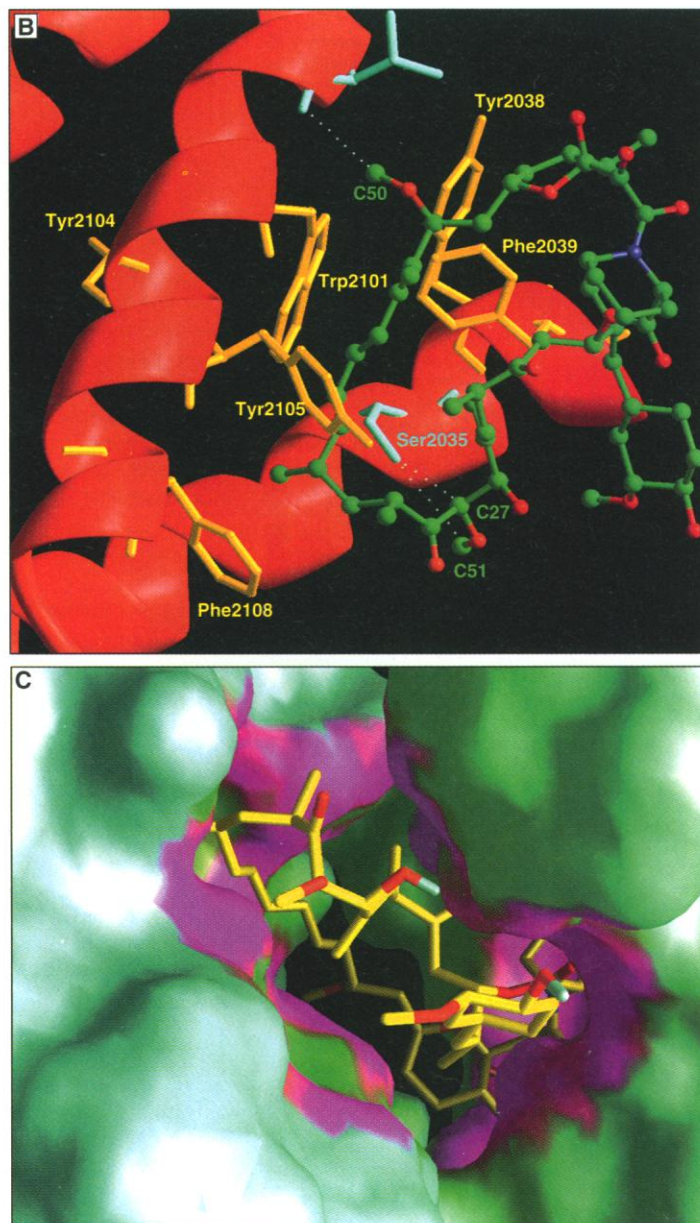


Fig. 2. Interactions of rapamycin with FKBP12 and FRB. **(A)** A LIGPLOT (32) rendering of the interactions of rapamycin with FKBP12 and FRB. Hydrogen bonds are shown by dashed lines (with lengths in angstroms), and hydrophobic interactions by surface dashes. **(B)** Close-up of the interactions of rapamycin (ball and stick) with the FRB domain of FRAP (red ribbon). Residue numbering is based on that for FRAP. **(C)** Complementarity plot of rapamycin with FKBP12 and the FRB domain of FRAP (33). High complementarity is indicated by purple. FKBP12 is on the right and the opening of the deep cavity where the pipercolinyl moiety is buried is visible. The FRB domain of FRAP is on the left, and the most deeply buried methyl group is shown disappearing into the FRB cavity.



FRAP) so that the FRB pocket is optimized for rapamycin binding.

Mutation of Ser²⁰³⁵ to Thr in FRAP renders the protein insensitive to the inhibitory effects of the FKBP12-rapamycin complex; the extra bulk of Thr²⁰³⁵ may prevent binding of rapamycin in the pocket (7) (Fig. 2). Mutations of Trp²¹⁰¹ and Phe²¹⁰⁸ also confer rapamycin resistance (29), and these residues also interact strongly with rapamycin (Fig. 2).

Our data provide a structural framework for understanding the rapamycin-based dimerization of FKBP12 and FRAP. Comparison of the FKBP12-FK506-calci-neurin structure (20, 21) with the FKBP12-rapamycin-FRB structure reveals different strategies for the two dimerization modes. Whereas FK506-induced dimerization features extensive protein-

protein interactions, rapamycin-induced dimerization does not. Because rapamycin-induced protein dimerization can form the basis for regulating gene transcription and other cellular processes (30), such structure-based modifications of the interaction might have important practical consequences. The structure also provides insights into structural features and possible regulation of the ATM family of proteins.

REFERENCES AND NOTES

- C. T. Keith and S. L. Schreiber, *Science* **270**, 50 (1995).
- V. A. Zakian, *Cell* **82**, 685 (1995).
- T. Hunter, *ibid.* **83**, 1 (1995).
- S. P. Jackson, *Curr. Biol.* **5**, 1210 (1995).
- E. J. Brown *et al.*, *Nature* **369**, 756 (1994).
- D. Sabatini, H. Erdjument-Bromage, M. Lui, P. Tempst, S. Snyder, *Cell* **78**, 35 (1994).
- E. J. Brown *et al.*, *Nature* **377**, 441 (1995).
- H. Tanaka *et al.*, *J. Am. Chem. Soc.* **109**, 5031 (1987).
- D. C. N. Swindells, P. S. White, J. A. Findlay, *Can. J. Chem.* **56**, 2491 (1978).
- S. N. Sehgal, H. Baker, C. Vezina, *J. Antibiot.* **28**, 727 (1975).
- C. Vezina, A. Kudelski, S. N. Sehgal, *ibid.*, p. 721.
- M. W. Harding, A. Galat, D. E. Uehling, S. L. Schreiber, *Nature* **341**, 758 (1989).
- J. J. Siekierka, S. H. Y. Hung, M. Poe, C. S. Lin, N. H. Sigal, *ibid.*, p. 755.
- S. L. Schreiber, *Science* **251**, 283 (1991).
- J. Liu *et al.*, *Cell* **66**, 807 (1991).
- D. M. Spencer, T. J. Wandless, S. L. Schreiber, G. R. Crabtree, *Science* **262**, 1019 (1993); P. J. Belshaw, S. N. Ho, G. R. Crabtree, *Proc. Natl. Acad. Sci. U.S.A.* **93**, 4604 (1996).
- G. D. Van Duyne, R. F. Standaert, P. A. Karplus, S. L. Schreiber, J. Clardy, *Science* **251**, 839 (1991).
- G. D. Van Duyne, R. F. Standaert, S. L. Schreiber, J. Clardy, *J. Am. Chem. Soc.* **113**, 7433 (1991).
- G. D. Van Duyne, R. F. Standaert, P. A. Karplus, S. L. Schreiber, J. Clardy, *J. Mol. Biol.* **229**, 105 (1993).
- C. R. Kissinger *et al.*, *Nature* **378**, 641 (1995).
- J. P. Griffith *et al.*, *Cell* **82**, 507 (1995).
- J. Chen, X. F. Zheng, E. J. Brown, S. L. Schreiber,

23. The expression and purification of recombinant human FKBP12 (19) and the FRB domain of human FRAP (22) have been described. Crystals of FKBP12-rapamycin-FRB were grown in 2 to 3 weeks at room temperature from hanging drops prepared from FKBP12 [10 mg/ml, in 10 mM tris-HCl (pH 8.0)], two equivalents of rapamycin (in methanol), and one equivalent of FRB [10 mg/ml, in 50 mM tris-HCl (pH 8.0)]. The well solution contained 20% (w/v) polyethylene glycol 8000, 10% methypentanediol, and 10 mM tris-HCl (pH 8.5). The rod-shaped crystals are orthorhombic, space group $P2_12_12_1$, with cell constants $a = 44.63$, $b = 52.14$, and $c = 102.53$ Å, and contain one ternary complex in the asymmetrical unit.
24. Data to a resolution of 2.7 Å (43,447 measurements of 6920 unique reflections, 98.5% complete, $R_{\text{sym}} = 0.071$) were collected from a crystal of dimensions 0.3 mm by 0.2 mm by 0.1 mm with the use of a San Diego multiwire area detector on a Rigaku RU-200 rotating anode x-ray source. Experimental phases were obtained from MR and SIRAS. MR with X-PLOR [A. T. Brünger, J. Kuriyan, M. Karplus, *Science* 235, 458 (1987)] and the FKBP12-rapamycin model (19) yielded a clear solution, but the resulting electron density map was noisy. A mercury derivative was prepared (2 mM HgCl_2 , overnight), and the two heavy atom sites were refined with PHASES [W. Furey and S. Swaminathan, *ACA Abstr.* 18, 73 (1990)]. Anomalous dispersion measurements were included in this data set and 16 cycles of solvent flattening were applied (PHASES). The resulting electron density map clearly showed the four-helix-bundle architecture of FRB. The FKBP12-rapamycin portion of the structure was well defined in the initial electron density map, and minor changes in the backbone of the 30s loop and some side chains were sufficient to fit the model. For the FRB portion, most of a polyalanine chain could be traced for the helical regions of the initial map. After several cycles of positional refinement (X-PLOR), loop regions could also be traced and the side chains assigned. CHAIN [J. S. Sack, *J. Mol. Graphics* 6, 244 (1988)] was used for model fitting and building the structure. A total of 95 residues in the FRB domain of FRAP (three residues in the NH_2 -terminal and two residues in the COOH-terminal regions showed no electron density and were not included), all residues of FKBP12, all atoms of rapamycin, and 23 water molecules were included in the final model. FRB residues are numbered according to FRAP numbering. The current R factor is 0.193 ($R_{\text{free}} = 0.299$) for data from 8 to 2.7 Å. The root-mean-square deviations of bond lengths and bond angles are 0.008 Å and 1.48°, respectively. The average temperature factors for all atoms and main chain atoms are 17.0 and 14.7 Å², respectively.
25. N. L. Harris, S. R. Presnell, F. E. Cohen, *J. Mol. Biol.* 236, 1356 (1994).
26. F. Lederer, A. Glatigny, P. H. Bethge, H. D. Bellamy, F. S. Mathews, *ibid.* 148, 427 (1981).
27. J. A. Findlay and L. Radics, *Can. J. Chem.* 58, 579 (1980).
28. X. F. Zheng, D. Fiorentino, J. Chen, G. R. Crabtree, S. L. Schreiber, *Cell* 82, 121 (1995).
29. M. C. Lorenz and J. Heitman, *J. Biol. Chem.* 270, 27531 (1995).
30. V. M. Rivera *et al.*, *Nature Med.*, in press.
31. M. Carson, *J. Mol. Graphics* 5, 103 (1987).
32. A. C. Wallace, R. A. Laskowski, J. M. Thornton, *Prot. Engin.* 8, 127 (1995).
33. A. Nicholls, K. Sharp, B. Honig, *GRASP Manual* (Columbia Univ. Press, New York, 1992).
34. We thank S. Ealick, J. Liang, and R. Gillilan for discussions. The Cornell work was funded in part by USPHS grant CA59021 (to J.C.) and the Harvard work by an Irvington Institute Fellowship (to J.C.) and USPHS grant GM38625 (to S.L.S.). S.L.S. is a Howard Hughes Medical Institute Investigator. Atomic coordinates have been deposited in the Protein Data Bank under the accession number 1FAP.

15 March 1996; accepted 15 May 1996

Long-Term Lymphohematopoietic Reconstitution by a Single CD34-Low/Negative Hematopoietic Stem Cell

Masatake Osawa,* Ken-ichi Hanada, Hirofumi Hamada, Hiromitsu Nakauchi†

Hematopoietic stem cells (HSCs) supply all blood cells throughout life by making use of their self-renewal and multilineage differentiation capabilities. A monoclonal antibody raised to the mouse homolog of CD34 (mCD34) was used to purify mouse HSCs to near homogeneity. Unlike in humans, primitive adult mouse bone marrow HSCs were detected in the mCD34 low to negative fraction. Injection of a single mCD34^{low/-}, c-Kit⁺, Sca-1⁺, lineage markers negative (Lin⁻) cell resulted in long-term reconstitution of the lymphohematopoietic system in 21 percent of recipients. Thus, the purified HSC population should enable analysis of the self-renewal and multilineage differentiation of individual HSCs.

CD34 is a marker of human HSCs, and all colony-forming activity of human bone marrow (BM) cells is found in the CD34-positive fraction (1). Clinical transplantation studies that used enriched CD34⁺ BM cells also indicated the presence of HSCs with long-term BM reconstitution ability within this fraction (2). After isolation of the human CD34 gene, the mouse homolog (mCD34) was isolated by cross-hybridization (3). To examine the expression and function of mCD34, we raised a monoclonal antibody (mAb), 49E8 [rat immunoglobulin G2a (IgG2a)], to mCD34 by immunizing rats with a glutathione-S-transferase (GST)-mCD34 fusion protein. This mAb stained BaF3 cells transfected with a full-length mCD34 cDNA but not mock-transfected cells (4). Murine cell lines such as PA6, NIH 3T3, M1, and DA1, shown by reverse transcriptase-polymerase chain reaction (RT-PCR) to contain mCD34 mRNA, were also stained by this mAb, indicating that 49E8, although specific for a GST-mCD34 fusion protein, could also recognize the native form of mCD34 as expressed on various cell types (4).

We next examined adult mouse BM for expression of mCD34. Four-color fluorescence-activated cell sorter (FACS) analysis was done after sequential staining of BM cells with a combination of lineage-specific mAbs to CD4, CD8, B220, Gr-1, Mac-1, and TER119, and then a mixture of mAbs to c-Kit (ACK-2), Ly6A/E (Sca-1), and mCD34 (5).

M. Osawa and H. Nakauchi, Department of Immunology, Institute of Basic Medical Sciences and Center for Tsukuba Advanced Research Alliance, University of Tsukuba, Tsukuba Science-City, Ibaraki 305, Japan. K.-i. Hanada and H. Hamada, Department of Molecular Biotherapy, Cancer Chemotherapy Center, Japanese Foundation for Cancer Research, Tokyo 170, Japan.

*Present address: KIRIN Pharmaceutical Research Laboratory, Gunma 371, Japan.

†To whom correspondence should be addressed.

Monoclonal antibody 49E8 reacted with $2.5 \pm 0.5\%$ (mean \pm SD) of total BM cells, with most of the positive cells occurring in the Lin⁻ fraction (Fig. 1A). More than 90% of the c-Kit⁺ Sca-1⁺ Lin⁻ cells previously shown to contain primitive HSCs (6) stained brightly with 49E8, whereas the remainder were low to negative (Fig. 1B). The frequency of mCD34⁺ c-Kit⁺ Sca-1⁺ Lin⁻ cells among total nucleated BM cells was $0.073 \pm 0.028\%$ (mean \pm SD, $n = 5$) and $0.004 \pm 0.003\%$ (mean \pm SD, $n = 5$), respectively.

To determine whether mouse HSCs express mCD34, we sorted subpopulations by FACS and examined their stem cell activity. Within the c-Kit⁺ Sca-1⁺ Lin⁻ population, the frequency of interleukin-3 (IL-3)-dependent colony-forming unit culture (CFU-C) per 200 cells was $20.0 \pm 3.9\%$ (mean \pm SD, $n = 8$) (7) for mCD34⁺ cells but only $0.16 \pm 0.4\%$ (mean \pm SD, $n = 8$) in the CD34⁻ fraction. Similarly, mCD34⁺ cells contained $14.1 \pm 3.4\%$ (mean \pm SD, $n = 15$) day 12 CFU spleen (CFU-S) per 200 cells, whereas in the mCD34⁻ fraction this value was $1.6 \pm 1.7\%$ (mean \pm SD, $n = 15$) (8). Thus, colony-forming activity was positively correlated with mCD34 expression among c-Kit⁺ Sca-1⁺ Lin⁻ cells. When these cells were cultured in the presence of both IL-3 and stem cell factor (SCF), however, 80% of mCD34⁻ c-Kit⁺ Sca-1⁺ Lin⁻ cells formed large multilineage colonies (7).

For in vivo analyses, c-Kit⁺ Sca-1⁺ Lin⁻ cells were fractionated into mCD34^{low/-} (Fr. 1), mCD34^{lo} (Fr. 2), and CD34⁺ (Fr. 3) subpopulations according to their mCD34 expression by FACS (Fig. 2A). Although 100 c-Kit⁺ Sca-1⁺ Lin⁻ cells were sufficient to radioprotect a lethally irradiated mouse, injection of 300 cells from either the Fr. 1 or Fr. 3 subpopulation (Fig. 2A) alone showed poor radioprotective ability (9). When cells